energies

MDPI

Article

Improving the Efficiency of Spark-Ignition Internal Combustion Engine Using a Novel Electromagnetic Actuator and Adapting Increased Compression

Jarosław Mamala [1,*], Bronisław Tomczuk [2], Andrzej Waindok [2], Mariusz Graba [1] and Krystian Hennek [1]

[1] Department of Vehicles, Faculty of Mechanical Engineering, Opole University of Technology, St. Mikołajczyka 5, 45-271 Opole, Poland
[2] Department of Electrical Engineering and Mechatronics, Faculty of Electrical Engineering Automatic Control and Informatics, Opole University of Technology, Prószkowska 76, 45-758 Opole, Poland
* Correspondence: j.mamala@po.edu.pl

Abstract: This paper presents an empirical study of a spark-ignition internal combustion engine with modifications made to increase its effectiveness. The modification was implemented bi-directionally in terms of changes to the compression ratio and changes to the engine's valve train. The compression ratio was increased by 2.3 units by design and a hybrid intake valve opening control was used in the engine's valve train. The hybrid control involved autonomous control of one of the inlet valves with a dedicated electromagnetic actuator. The designed electromagnetic actuator was mounted downstream of the single-cylinder engine's intake system's modified camshaft to control the effective compression pressure build-up. Field calculations were carried out for the electromagnetic actuator's design variants and its current characteristics were determined. The multivariate calculations were carried out in order to find the quasi-optimal geometry of the actuator. The width and height of magnetic field coils and the dimensions of the stator poles were changed, while maintaining the same external dimensions of the actuator to enable its mounting in the cylinder head system. In the next step, the prototype of the actuator was made and placed on the combustion engine in order to conduct the experimental investigations. The work was aimed at improving the internal combustion engine's efficiency at the low load range, as this is load range in which it has low efficiency despite it being the most often used during normal vehicle operation. The original measurement stand was prepared, and many tests were carried out in order to investigate the influence of the electromagnetic valve on the combustion engine characteristic. This improved the internal combustion engine's efficiency at its low-load range by up to 25%. Both calculation and measurement results are presented in form of graphs.

Keywords: electromagnetic actuator; combustion engine fuel conversion efficiency; compression ratio; valve controlling

check for updates

Citation: Mamala, J.; Tomczuk, B.; Waindok, A.; Graba, M.; Hennek, K. Improving the Efficiency of Spark-Ignition Internal Combustion Engine Using a Novel Electromagnetic Actuator and Adapting Increased Compression. *Energies* **2023**, *16*, 5355. https://doi.org/10.3390/en16145355

Academic Editor: Venera Giurcan

Received: 24 May 2023
Revised: 23 June 2023
Accepted: 11 July 2023
Published: 13 July 2023

1. Introduction

Internal combustion engines of vehicles equipped with classic propulsion systems operate mainly in the range of partial loads, where the engine efficiency is significantly lower than its maximum [1]. This fact applies especially to urban driving, where crankshaft speeds are much lower than in motorway driving, and its changes are more frequent and intense. The same applies to the engine load variability in the vehicle's drive unit. Hence, the engine's overall efficiency in variable conditions depends on the load and crankshaft speed, but in instantaneous operating conditions, the efficiency depends on the temporary maximum compression ratio in the cylinder. Maintaining the highest compression ratio possible under given conditions for traditional internal combustion engines is difficult due to limitations in the air mixture's combustion process in the cylinder, including the occurrence of engine knocking. The engine's maximum peak compression ratio can be adjusted in several ways. Currently, the most popular method of changing the

cylinder's pressure is to change the throttle valve opening angle, which limits the flow of the fuel–air mixture to the engine as well as the pressure increase. Flow reduction with a closed or partially opened throttle valve in the intake manifold causes the engine to run with a large negative charge exchange loop. This leads to a reduction in the engine's compression ratio, which in turn reduces its maximum efficiency. One way to solve this issue is to use an internal combustion engine turbocharger, which is often insufficiently efficient at low speeds. It would therefore be preferable to ensure a high compression ratio (CR) at low-load conditions and a low CR at high-load conditions, which aids the aforementioned methods of adjusting the maximum compression ratio. It was the engine's variable compression ratio that prompted the authors to build an electromagnetic actuator to control the compression ratio in valve train. As the internal combustion engine is still the most popular source of power for vehicle drive units, this topic is addressed in many scientific elaborations [2,3], where the issue of inadequate use of engine power in a passenger car's drive unit is described extensively in terms of its low loads and improved charge exchange. The introduction of solenoid valves, so-called live valves, which do not have a kinematic connection with the engine's crankshaft, provided a new degree of freedom into the control system. In this case, it is possible to control the valve's opening time and lift, significantly affecting the charge exchange and cylinder pressure build-up. In his paper [4], Theobald presented an empirical study carried out on a single-cylinder engine, where the focus was on optimizing the valve train's operation by controlling the opening time at 1500 RPM under varying load conditions with a stoichiometric fuel–air mixture. Changing the valves' opening angles and timing relative to the top dead center (TDC) enabled the introduction of internal exhaust fume recirculation in the engine's cylinder. It was shown that the introduced changes had a positive effect on power and reduction in primary emissions. The operation of a valve train based on electromagnetic actuators with a moving coil is the subject of elaboration [5], in which attention was paid to the system's current efficiency by changing the valve opening and closing cycle, and the resulting issue of the valve hitting the head seat. The current efficiency was assessed based on the valve motion speed and the coil's electromagnetic force. The paper's results indicate that the use of adequately programmed controllers provides a better current efficiency. This topic is also addressed in papers [3,6], which focus not so much on internal combustion engine efficiency, but on control algorithms using programmable electromagnetic actuators, which were demonstrated to reduce electromagnetic interference with the use of adaptive Nelder–Mead or Fuzzy Logic valve control algorithms, especially in the actuator start-up phase. The efficiency of an internal combustion engine with its valve train equipped with electromagnetic actuators was highlighted in paper [6], which features a comprehensive study of its duty cycle for a homogeneous charge compression ignition (HCCI) with fuel direct injection and a turbocharging system. Internal combustion engines of this type are still in the advanced testing phases, but the engine's tests at full load and with turbocharging at 400 to 650 kPa demonstrated a 6% deterioration in the cylinder's indicated mean effective pressure (IMEP) and an increase in nitrogen oxide emissions to approx. 8 g/kWh. During testing, attention was paid to the engine's lower load ranges, where fuel injection combined with extended intake valve opening time, affecting the negative charge exchange loop, will have a beneficial effect on the engine's operating stability and uniformity. In our own research [1], attention was paid to the possibility of controlling combustion pressure using a solenoid valve in the engine's operating field, reducing fuel consumption in the engine's low-load range and speed of no more than 1250 RPM by up to 12%.

Nevertheless, the field for improving the overall efficiency of internal combustion engines is not yet closed and opportunities to improve them should be sought in many areas, one of which is, for example, reduction in friction losses in internal combustion engines. New lubricants [7] or the design of the elements of the piston–rings–cylinder system is of great importance [8]. In these two works, the authors noted that increased engine torque at low crankshaft angular velocity gives a consequence of an increase in the mean unit pressure distribution of the piston rings. This effect applies especially to the

upper sealing ring as the expansion stroke starts. It affects the formation of an oil film by slip reduction. Improving the cooperation of these elements also means improving the overall efficiency of the internal combustion engine by reducing its mechanical losses. One of the key technological challenges of using electromagnetic actuators is a current efficiency that enables such a system to operate on the vehicle's power. Therefore, this paper presents a hybrid system that is a combination of a classic valve train with an electromagnetic actuator to control the cylinder's combustion pressure, but for an internal combustion engine with an increased compression ratio compared to a factory engine.

2. Motivation for Taking Up the Topic

The information presented demonstrates that the use of electromagnetic actuators in the engine's valve train provides additional freedom into the engine's power control system—particularly under the conditions of the engine's forced operation resulting from the vehicle's implemented speed profile, where the internal combustion engine operates in conditions that are far from optimal. The work [9] describes the benefits of using power-controlled engines with a variable compression ratio tested in NEDC and real WLTP synthetic driving cycles. Significant benefits have been demonstrated from these systems, resulting in a 7.5% reduction in fuel consumption. The research described in [10] also indicates a great potential for the use of variable compression ratio engines; it even indicates the potential to compete with electric motors used to drive passenger cars. For the tested engine, when the compression ratio was increased from 9.5 to 10.1, fuel consumption (FC) was reduced by 6–8%, and efficiency increased by 3.5% at 75% engine power load. An internal combustion engine's optimal operation is in the range of 80–90% of its torque load and 20–40% of its crankshaft speed range, which is most often in the range of 2000 to 3000 RPM. At the same time, the internal combustion engine should operate at its set crankshaft speed, which usually translates into the vehicle's driving speed of 70–90 km/h [1,11]. The internal combustion engine's highest efficiency is achieved under such conditions and these values exceed the 44% limit in modern engines [12]. For this reason, the vehicle's mileage fuel consumption is lowest, and its consumption is higher for both lower and higher driving speeds in the rest of the range. However, engine efficiency is in the range of 12–19% under everyday operating conditions, especially in the city, when driving speeds are significantly lower and generally do not exceed 40 km/h [1]. At the same time, under such operating conditions, the internal combustion engine runs for around 60% of its operating time, assuming a normal driving style. In the rest of the car's speed range, both lower and higher speeds result in an increased fuel consumption. The key solution is to increase the engine's efficiency, which is simple in theory, because definition (1) states that its efficiency depends on the compression ratio.

$$\eta_{t\ Otto} = 1 - \frac{1}{\varepsilon^{k-1}} \tag{1}$$

where ε is the compression ratio, k is the specific heat ratio [1].

Higher efficiency results in lower fuel consumption; therefore, paper [13] presents the desired compression ratio variability compared to the engine's overall characteristics. Hence, many research facilities work on variable compression ratio engines; however, such engines are still being tested, as in the case of HCCI engines. The work [14] presents a study on a single cylinder direct injection CI engine's work, while varying the compression ratio (at the values of 18, 17, and 16) and varying the load. The influence of the reduction in the compression ratio on performance and combustion parameters was analyzed. As the compression ratio was reduced, the following occurred:

- a decrease in break thermal efficiency and peak cylinder pressure was noted,
- an increase in break specific fuel consumption, ignition delay period, and exhaust gas temperature was observed.

The authors of the article [15] present two Saab concepts: Saab Variable Compression (SVC) and Saab Combustion Control (SCC). The aim of both new systems is the reduction of fuel consumption and parasitic losses.

In paper [16], the technology, working principle, and advantages of the VC-T (Variable Compression Turbo) engine are presented. The VC-T engine' s compression ratio (CR) is adjustable between 8:1 and 14:1, which makes it possible to increase the efficiency by using high CR at idle and low driving velocities and increase the performance by lowering the CR while driving with high acceleration dynamics or heavy engine loads. In [17], a new variable compression (VCR) engine with a multiple-link piston-crank system was proposed. The desired CR in given operating conditions is set by varying the motion of the piston at TDC. This mechanism is installable without generally changing the size and weight of the engine. The authors prove that fuel consumption can be decreased and the engine's power can be increased simultaneously by using high CR and exhaust gas recirculation (EGR) in low-load conditions and low CR and high boost pressure in high-load conditions. The impact of the change in the piston movement has on fuel economy and maximum power at partial load is presented. Furthermore, the use of higher compression ratios involves a disruption in the combustion process in the cylinder through the occurrence of engine knocking. Engine knocking is detrimental due to toxic gas emissions derived from combustion, but it is also detrimental for the engine's durability. A very important technical solution used in the world of technology to control the operation of internal combustion engines is the concept described in paper [18], involving a significant increase in the intake valves' opening angle in the intake stroke, which affects the negative charge exchange loop. This allowed for making a reference to Atkinson's work [19], who improved the engine's efficiency by changing the negative charge exchange loop. Keeping in mind the technical solutions outlined above, the authors of this paper focused on an internal combustion engine with a higher compression ratio by design, i.e., a permanently increased compression ratio in its entire operating area, adapting the combustion pressure in the cylinder to the engine's current load via an electromagnetic actuator powering a single intake valve. This enabled achieving a combustion pressure in the cylinder that corresponded to a high compression ratio at low loads and an increased intake valve opening angle at higher loads. The opening angle increase reduces the volume of the stoichiometric mixture that takes an active part in the combustion process, lowering the combustion pressure and preventing engine knocking. The combustion pressure reduction is comparable to the combustion pressure of an internal combustion engine with a factory compression ratio, thereby achieving effective compression control in the cylinder. Therefore, the authors assumed the main goal of the work in the form of carrying out the electromagnetic actuator modelling process, was mounted downstream of the single-cylinder engine's intake system's modified camshaft to control the effective compression pressure build-up. Field calculations were carried out for the electromagnetic actuator's design variants and its current characteristics were determined for the designed actuator. The width and height of magnetic field coils and the dimensions of the stator poles were changed, while maintaining the same external dimensions of the actuator to enable its mounting in the cylinder head system. The entire research was to lead to improving the internal combustion engine's efficiency at the low load range, where it has low efficiency.

This manner of engine operating cycle control required implementing a modification of the valve train through its hybridization, combining a classic cam valve train with an electromagnetic actuator. This reduced the actuator's current demand but, at the same time, necessitated the designing and selection of the tested actuator's design parameters, which is described below.

3. Effective Compression Ratio

The maximum compression ratio increase is a basic indicator of an internal combustion engine's operation that characterizes its operating capacity and is often related to the engine's compression ratio. In internal combustion engines, the maximum compression

ratio not only depends on its compression ratio, but also on the throttle valve opening angle, which determines the cylinder's supply of fresh charge in the compression stroke. The compression ratio defined this way can be demonstrated in the form of the equation provided below (2):

$$\gamma = \frac{p_{e\ max}}{p_{min}} \tag{2}$$

where $p_{e\ max}$—maximum effective pressure [Pa], p_{min}—intake pressure [Pa] [1].

The effective compression ratio can be adjusted in a number of ways, including changing the throttle valve opening angle or using a turbocharger. However, in order to maximize the engine's efficiency, it is advantageous to have the additional effect of pump loss reduction during the intake stroke. This combination allows for achieving the engine's maximum efficiency at the given design parameters. In this case, the authors used an internal combustion engine with a structurally increased compression ratio and a valve train modified by the addition of an electromagnetic actuator to control one of the intake valves. The basic characteristics of the effective compression ratio for a single-cylinder internal combustion engine are shown in Figure 1.

(**a**) (**b**)

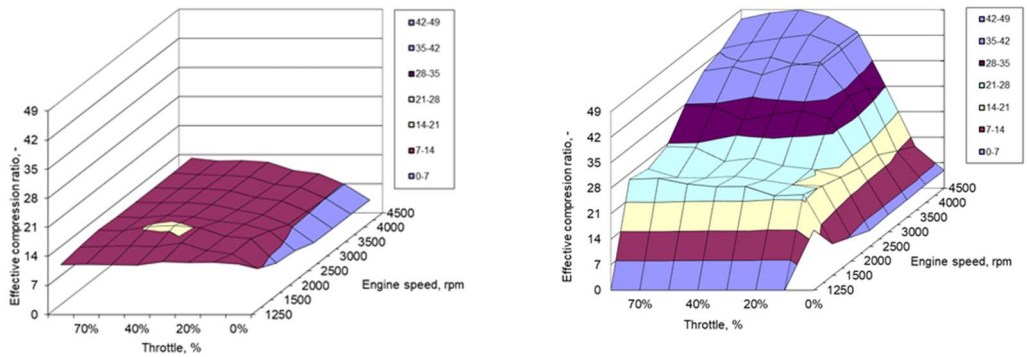

Figure 1. Basic characteristics of the test engine's effective compression ratio: (**a**) ignition switched off, (**b**) normal operation.

A comparison of the engine's efficiency characteristics with the ignition switched off (Figure 1a) and with its efficiency with the ignition switched on (Figure 1b) shows significant qualitative and quantitative differences. Figure 1b demonstrates that the efficiency increases significantly above 2500 RPM. At low engine speeds and engine loads, the new electromagnetic actuator is synchronized with the second intake valve. In this way, in the timing system of the internal combustion engine, there are no changes in its work cycles (valves opening and closing) [1,20]. Under these conditions, the internal combustion engine has a high compression ratio, and the effective compression ratio is only controlled by the throttle in the intake manifold. As the engine's load increases, the electromagnetic actuator takes longer to open the intake valve, thereby controlling the effective compression ratio [1,20]. Such electromagnetic actuators are used in many applications, e.g., for transportation [21,22], wave–energy conversion [23], and linear engines [24,25]. Their application eliminates the conversion of rotary motion into linear motion in many drive units, i.e., in combustion engines [26], pumps [27], and high-compression engines [28]. Linear electromagnetic actuators are used due to their high reliability, dynamic properties, and electro-mechanical parameters [29,30]. In case of the electromagnetic actuators for valve driving, there are different solutions investigated in the literature. In [31] the hybrid construction consisting of two different permanent magnet actuators is presented. The composite construction is relatively complicated. In [32], an electromagnetic linear actuator connected in series with the magnetorheological buffer is investigated. The buffer is used to reduce the seat velocity, but it also increases the switching time. A hybrid permanent

magnet electromagnetic valve is presented in [33]. It is characterized by a simple construction and relatively low energy consumption. However, its disadvantage is a relatively long switching time. In [34], a bi-stable actuator with permanent magnets was presented. It is characterized by a good dynamic properties, simple construction, and low energy consumption. Its disadvantage is the use of permanent magnets, which could suffer under relatively high temperature arising in the combustion engine.

In the presented work, a four-stroke single-cylinder test engine was equipped with an electromagnetic actuator and its control system, allowing for valve train-independent inlet valve action (Figure 2). As an actuator, a novel construction without permanent magnets was implemented. The elimination of permanent magnets is important due to the reliability of the actuator.

(**a**) (**b**)

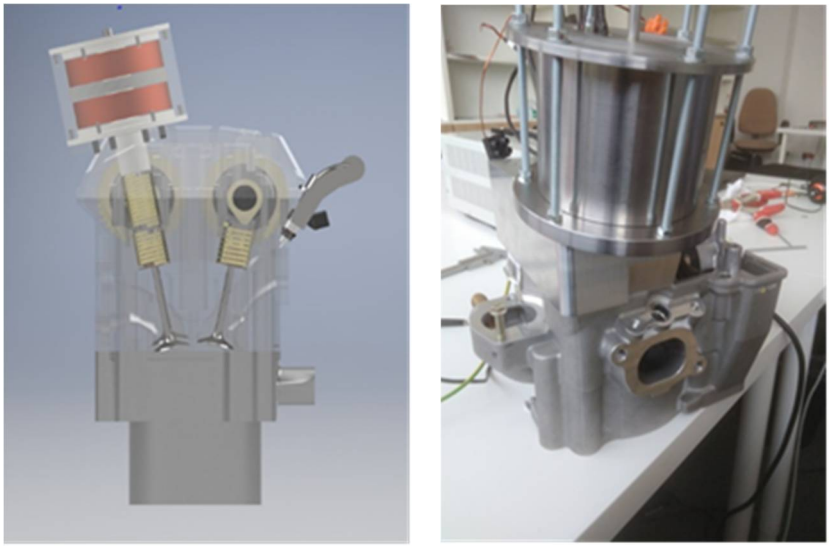

Figure 2. Single-cylinder internal combustion engine equipped with an electromagnetic actuator: (**a**) cylinder head with actuator, (**b**) photograph of the cylinder head with the actuator.

4. Electromagnetic Actuator Parameters

Technical literature features many elaborations on electromagnetic actuators used for powering valves in an internal combustion engine, including patented solutions [35,36] and commercial solutions for direct application [37]. However, electromagnetic actuators are still characterized by multiple properties, a varied selection of parameters, and are the subject of many studies carried out in different research centers. The presented papers are multi-faceted and, for example, concern the selection of design parameters [38], describing the theoretical issues with regard to the designing of such an actuator, which were verified during tests on a single-cylinder internal combustion engine's valve train, with attention being paid to the issue of the solenoid valve's needle protrusion, determining the opening cross-section in the valve seat during the suction stroke. The main, priority goal of the designed actuator was to obtain high dynamics, high force, and low dissipation power loss, and thus geometric dimensions at this stage of the work had less priority. The non-linear model was used to present and discuss the control strategy based on computer simulations and empirical studies to further improve the actuator's design. In paper [39], attention was paid to the dynamics of linear electromagnetic actuators and the authors presented a simple model to study the effect of eddy currents on the dynamics of the protrusion of the needle that moved the valve. The dynamics were modelled using the finite element method, which implements the non-linear properties of the magnetic material with a modified Weibull distribution. The model is voltage-controlled. The results of the finite element method (FEM) simulation were compared to laboratory tests, thereby achieving comparative needle acceleration at real-life loads. One of the challenges of electromagnetic actuators used in

an internal combustion engine's valve train is the robust valve needle movement control to achieve smooth closure under different operating conditions. This issue was addressed in paper [40], which describes laboratory tests of the effects of different algorithms on the valve stalling and valve seat impact. The study involved testing of two valve movement controllers in a single-cylinder internal combustion engine. The controllers were compared in their state of transition from an open exhaust valve to a closed exhaust valve at large combustion pressure fluctuation. A new control algorithm that operates reliably over a wide range of operating conditions was presented. The analysis demonstrated that the electricity consumed by the cam-less valve train is comparable to the energy of an equivalent conventional valve train based on low-friction camshafts. Papers [33,41] describe a hybrid electromagnetic actuator design with a permanent magnet and electromagnetic coils installed together, which differs significantly from existing electromagnetic actuators that are used in valve trains; the actuator's strength is the reduced force required for actuation. A magnetic flux density simulation was carried out to optimize the actuator, and its results show that such an actuator with soft-closing control can fully satisfy the valve dynamics of spark-ignition engines. In paper [38], an attempt was made to design an electromagnetic actuator with an unusual cuboid structure, in which the movable pin consists of flat permanent magnets arranged alternately with ferromagnetic spacers. The construction of the stator includes six coils forming three pairs of poles, which makes this electromagnetic actuator similar to a linear reluctance motor. At the same time, it is an actuator that generates zero force from the neutral position and the rated force varies in the range of 600–650 N. This is a typical value for this actuator and the advantage of this solution is the low mass of the moving pin ensuring high dynamics and low energy consumption. The disadvantage is the durability of the pin due to the material used (magnets lose their properties under the influence of vibrations).

The above considerations and the authors' experience in building linear actuators led them to work on the design of an actuator dedicated for a single-cylinder spark-ignition engine operating in a hybrid valve train with three cam-driven valves and one electrically driven valve. A construction of an axisymmetric electromagnetic actuator with a moving spindle in the form of a ferromagnetic cylinder was proposed, and two-state operation was assumed. This is of great importance in the design of the actuator because it can generate force in both directions of movement, as well as in the technology of the actuator. Two structures were considered: one solution based on coils [42], and one on coils with a permanent magnet [36]. The basic calculations for the actuator without permanent magnets are presented below. The authors chose a tubular design for the actuator. It is the most effective design in terms of the ratio of electromagnetic force to the movable component's mass [43]. Figure 3 shows the actuator's main dimensions. This model was used in the simulation program.

The actuator consists of a stator and drive unit. A preliminary number of winding turns was assumed in the first phase of calculations. The polarization field is excited by the currents in the external coils (DC coils). Their main task is to keep the drive unit in stable extreme positions (valve opened and closed). Each coil has N_1 = 72 turns and are wound separately. The control electromagnetic field is excited by two internal coils with N_2 = 118 turns each. The coils are connected in series. The main task of these coils is to create a magnetic field to move the drive unit to a different stable position. The number of turns was calculated based on the coils' dimensions and the assumed non-insulated wire cross-section (3 mm^2).

The stator consists of the main tube-shaped external part as well as the bottom and upper covers, which form the main magnetic circuit. The drive unit consists of two parts: the magnetic core's movable part and shaft. In the magnetic field analysis, the authors took into consideration the Austenitic steel shafts. Table 1 presents the initial dimensions for the actuator's variant calculations.

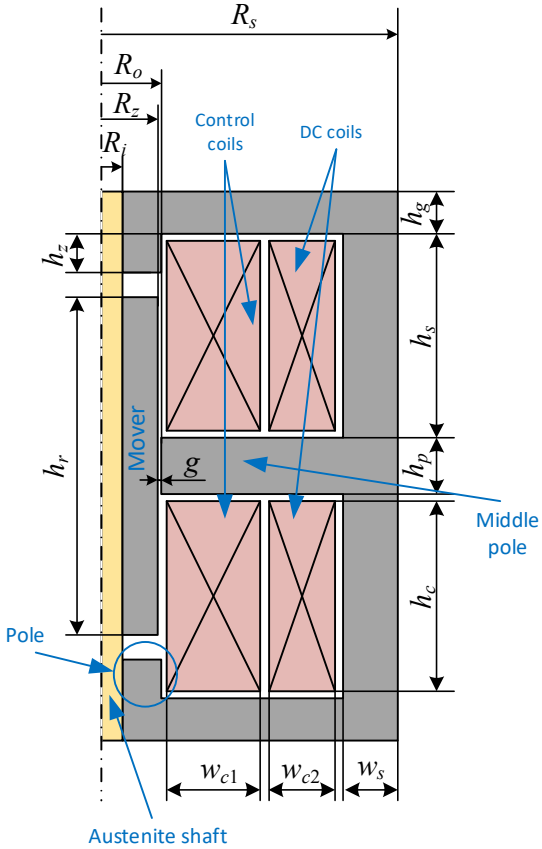

Figure 3. Actuator dimensions shown in the axial cross-section. Model used in the simulation program.

Table 1. The actuator part's initial dimensions (in mm).

Parameter	R_s	R_o	R_z	R_i	h_z	h_g	h_p	h_r
Value	42	8.5	8	3	8	6	8	40
Parameter	g	h_c	w_{c1}	w_{c2}	w_s	h_s		
Value	0.5	27	16.5	10	4	29		

4.1. Mathematical Model for the Magnetic Field Analysis

The magnetic field distribution was obtained with the aid of an FEM software. To simplify the field analysis, the mathematical model omitted the eddy currents, and the magnetic field was considered as stationary. Furthermore, the authors omitted the fact that the manufacturing process slightly changes the magnetic properties of the core material. Thus, the magnetic air gap value was slightly increased in the calculated model. On the other hand, the authors took into account the non-linear nature of the flux density changes in field intensity function.

The analysis was performed with the assumption that the 3D magnetic field issue can be reduced to a 2D issue, thereby significantly simplifying the model's mathematical description and reducing the calculation time. This is due to the symmetry of the designed electromagnetic actuator because construction details do not significantly affect the distribution of the magnetic field. This results from the studied object's geometry, because the design details are not considerably affecting the magnetic field's distribution. This allows the two-dimensionality to ensure that the calculations are much more economical and convenient.

As in paper [43], the author assumed the non-linear nature of the ferromagnetic core's fragmentary magnetization, which allowed them to describe the magnetic field by using the following formula:

$$\nabla \times \left(\frac{1}{\mu(B)} \nabla \times A \right) = J. \tag{3}$$

The field analysis was based on calculating the magnetic vector potential A [23], which only consists of the vector's polar component (A_φ). Due to the cylindrical symmetry of the proposed tubular actuator, the authors used the polar coordinate system. The use of the vector potential's polar component is used (as a find function) [43], and the magnetic field can be described by using the following partial differential equation (PDE):

$$\frac{\partial}{\partial r}\left(\frac{1}{\mu(B)} \frac{\partial A_\varphi}{\partial r} \right) + \frac{1}{r \cdot \mu(B)} \frac{\partial A_\varphi}{\partial r} + \frac{\partial}{\partial z}\left(\frac{1}{\mu(B)} \frac{\partial A_\varphi}{\partial z} \right) - \frac{1}{\mu(B)} \frac{A_\varphi}{r^2} = J_\varphi \tag{4}$$

where $\mu(B)$ is the magnetic material's non-linear permeability; J is the current density in the excitation windings [43].

Taking into account the potential's rotation operator, it is possible to calculate the components of the magnetic flux density vector

$$B = -\frac{\partial A_\varphi}{\partial z} 1_r + \frac{1}{r} \frac{\partial (r A_\varphi)}{\partial r} 1_z \tag{5}$$

Based on the knowledge of magnetic field distribution, it is possible to determine the field's integral parameters, especially including the magnetic force generated by the actuator. When the ferromagnetic component is moving, the force can be calculated from the changes in the energy or the magnetic stress tensor. The force is determined by using Maxwell's stress tensor on the edge of the moving ferromagnetic area [43]:

$$F_e = \int_\Omega f d\Omega = \oint_\Gamma \overset{\leftrightarrow}{T} \cdot d\Gamma, \tag{6}$$

where,

$$\overset{\leftrightarrow}{T} = \begin{bmatrix} \mu\left(H_r^2 - \frac{1}{2} H^2 \right) & \mu H_r H_z \\ \mu H_r H_z & \mu\left(H_z^2 - \frac{1}{2} H^2 \right) \end{bmatrix} \tag{7}$$

For non-linear characteristics $B(H)$ of the core elements, the magnetic force can be determined using the scalar product of the magnetic intensity vector and the corresponding magnetic flux density vector, at each point of the core.

$$F_e = \frac{1}{2} \oint_\Gamma (H(B \cdot n) + B(H \cdot n) - (H \cdot B) n) \cdot d\Gamma \tag{8}$$

Another important integral parameter that affects the actuator's inductance is the magnetic flux Ψ related to all coil windings. It is possible to calculate the product of the normal component B_n and the surface area of each component in the area enclosed by the winding's contour for the kth coil winding. The integration of such products over each coil winding and summation of the integrals allow for the determination of the flux linkage

$$\Psi = \sum_{k=1}^{N} \int_S B_n dS_k, \tag{9}$$

where S_k—area enclosed by the kth coil [43].

The coil's dynamic inductance was calculated based on the definition as a partial derivative of the flux linkage associated with the coil in relation to the current

$$L_d = \frac{\partial \Psi}{\partial i} \tag{10}$$

This software utilized formulas 3 to 10 in order to inspect the field at arbitrary points, and to evaluate a number of different integrals and determine various quantities of interest along the user-defined contours (Figure 2). The non-linear curve $B(H)$ was included in the model. The Dirichlet boundary condition was assumed for the calculation area's outer boundaries

$$A_\varphi = 0 \tag{11}$$

4.2. Results of the Variant Calculations

With additional cooling of the actuator's main body (external magnetic core), the authors assumed relatively high current densities J = 10 A/mm^2 for all coils. The initial height h_c was the same for both the polarization and control coils. The initial widths of the control coil w_{c1} and of the bias coil w_{c2} are presented in Table 1. The same current intensity I = 30 A in the bias and control coils was assumed for the preliminary dimensions. The number of coil windings was changed depending on the wire dimensions (a copper wire with 1 mm by 3 mm cross-section was assumed).

4.2.1. Influence of the Coil Width on the Magnetic Force

Different winding cross sections were assumed for the variant calculations. Specific magnetic forces were calculated with the assumption of constant current density in the coils. These forces included the average value F_{AV}, maximal value F_{max}, and density f_m [N/kg] of the maximal force, based on the drive unit's mass.

Figure 4 shows graphs comparing two of the above-mentioned forces with the ratio of w_{c2} and $w_c = w_{c1} + w_{c2}$. The remaining dimensions are given in Table 1. It is evident that the forces achieve their maximum values when the width w_{c1} approaches w_{c2} and reaches half of the core window.

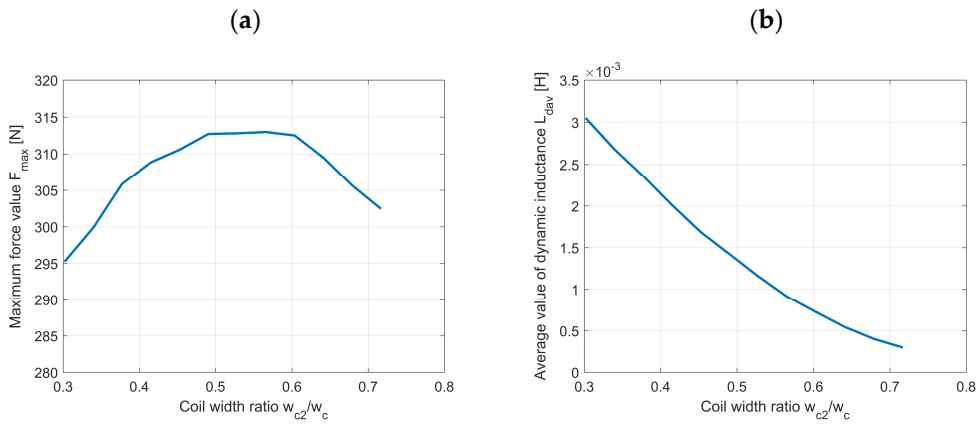

Figure 4. Maximum force (**a**) and average dynamic inductance (**b**) versus the ratio of the coil width w_{c2} and the two coil's total width w_c.

The peak value in the graph presenting the maximum thrust versus the w_{c2}/w_c ratio (Figure 4a) is achieved when the ratio is in the range of 0.5 and 0.6. For this range, the average dynamic inductance L_{dav} is between 1.7 mH and 1.4 mH (Figure 4b). The inductance decreases along with an increase in the w_{c2}/w_c ratio. Its smallest value is the most advantageous for the actuator's dynamics. Taking into account the magnetic force, the optimum condition is when the widths of the polarization and the control coils are nearly the same.

4.2.2. Optimum Height h_z of the Extreme Poles

The optimum height h_z of the external ferromagnetic core is very important for the actuator's thrust force and dynamics. This was the reason for studying the impact of height on the maximum force (F_{max}) and average dynamic inductance value—L_{dav} (Figure 5). The graphs show the dependence of the force and inductance changes on height h_z (Figure 5).

A height ranging from 5 to 15 mm is best for the design. An increase in height in the aforementioned range does not considerably affect the maximum force or the average dynamic inductance L_{dav} (Figure 5b). Taking into account the optimum force value (Figure 5a), the optimum height is h_z = 10 mm.

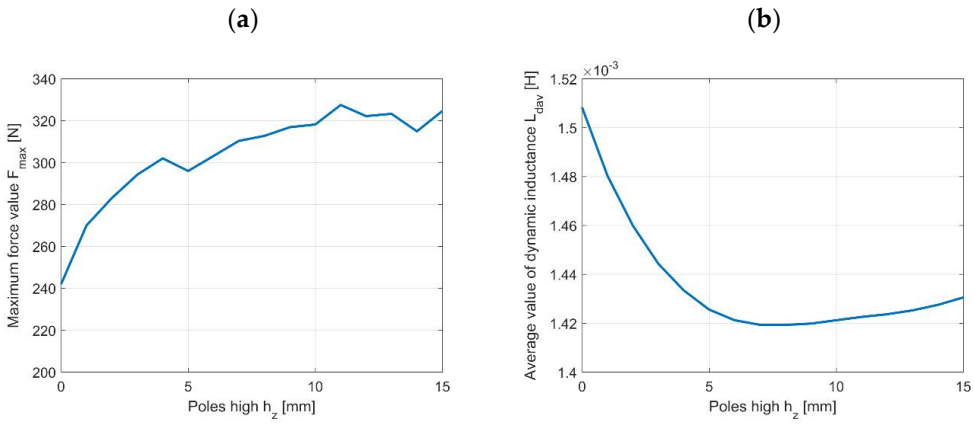

Figure 5. Dependency of maximum thrust (**a**) and average dynamic inductance (**b**) on the extreme poles' height h_z.

4.2.3. Impact of the Drive Unit's Radius (R_z)

Very strong changes in the magnetic field's integral parameters occur when the moving ferromagnetic core's volume increases. The graphs in Figures 6 and 7 show the impact of changes in the drive unit's radius R_z on the actuator's selected parameters. Due to the constancy of the actuator's volume, it is evident that an increase in the radius causes a decrease in the coils' width.

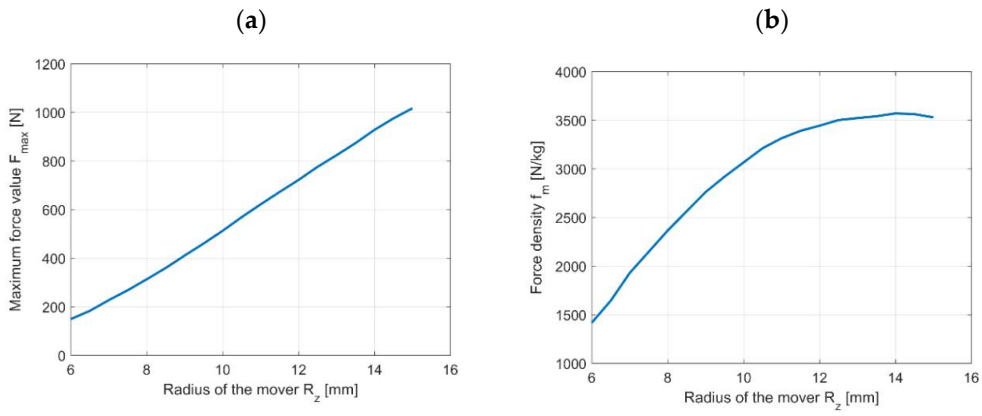

Figure 6. Dependency of maximum thrust (**a**) and maximum force density (**b**) on the radius R_z.

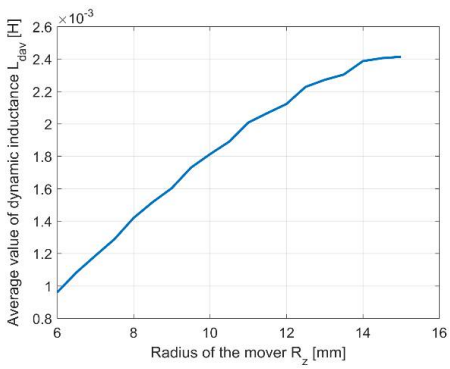

Figure 7. Dependency of average dynamic inductance on the radius R_z.

Taking into account the actuator's real dimensions, the radius R_z was being changed within the range from 6 mm to 15 mm. The maximum force F_{max} [N] and the maximum force density f_m [N/kg] are presented in Figure 6. A five-fold increase in maximum force is achieved at a two-fold increase in the radius. On the other hand, a 1.5 increase in force density is achieved at a two-fold increase in the radius (R_z = 14 mm) (Figure 6b). This is a result of the simultaneous increase in the force and the drive unit's mass.

The obtained results show that the drive unit's radius significantly affects the average dynamic inductance L_{dav} (Figure 7). An increase in the radius R_z causes an increase in inductance L_{dav} (Figure 7). However, an increase in the radius causes a reduction in magnetic flux density, which results in a smaller increase in the coil-linked flux (for the greater R_z) and a smaller increase in inductance.

4.2.4. Impact of the Central Pole's High h_p

Figure 8 shows the dependency of the maximum force F_{max} and the average dynamic inductance L_{dav} on the various dimensions (h_p) of the central pole. The ferromagnetic pole is an important part of the magnetic circuit. Its dimension was changed in the range from 8 mm to 16 mm. The height of the coils should also be changed based on height h_p because the actuator's external dimensions should be constant. Figure 8 shows that the thrust and dynamic inductance are slightly reduced depending on the central pole's height h_p.

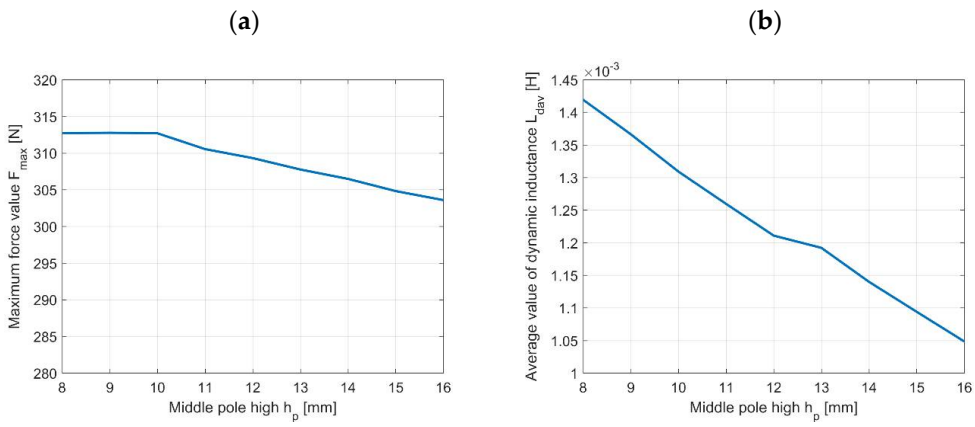

Figure 8. Dependency of maximum thrust (**a**) and average dynamic inductance (**b**) on h_p.

The actuator's designing phase featured measurements of the inlet valve spring force, which amounted to around 400 N. Moreover, as the valve is opened by the actuator, additional air pressure is applied during the compression stroke. Hence, the focus was placed on achieving the actuator's maximum force and high dynamics. The final assumed dimensions of the actuator are given in Table 2.

Table 2. The actuator final dimensions (in mm).

Parameter	R_s	R_o	R_z	R_i	h_z	h_g	h_p	h_r
Value	50	13,5	13	3	10	10.5	8	38
Parameter	g	h_c	w_{c1}	w_{c2}	w_s	h_s		
Value	0.5	28	12.5	12.5	8.5	30		

5. Test Results

The first step in the development of the control system was the identification of signals from the crankshaft, camshaft, fuel injection control, and cylinder pressure sensors. The recorded data are presented in Figure 9.

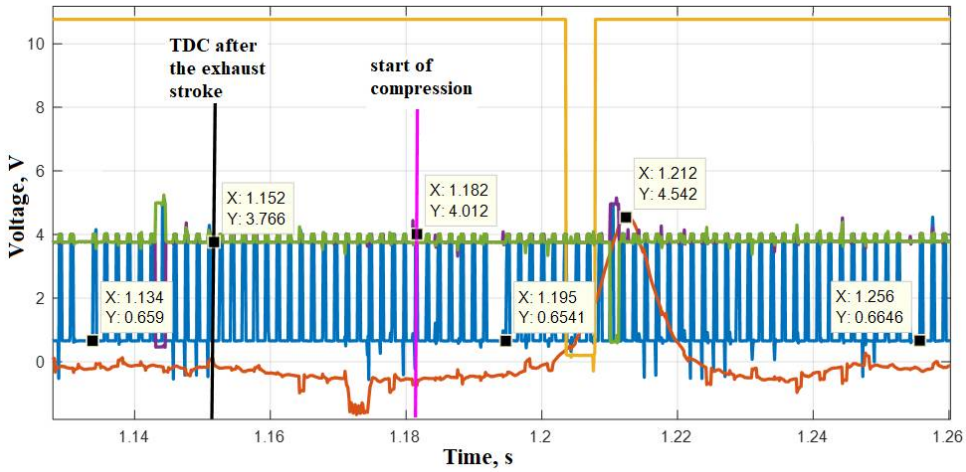

Figure 9. Signals recorded from the test engine, blue—crankshaft, orange—camshaft, green—ignition, violet—fuel injector, red—cylinder pressure.

The pink line shown in the above Figure marks the piston's bottom dead center and is the point at which the air compression in the cylinder begins, and at which the designed valve begins opening (Figure 9).

The control system was built based on a modular platform, the heart of which was a 1.33 GHz Dual-Core CPU processor operating with 2 GB DRAM memory and on the Kintex-7 160 T FPGA chip. The advantage of this system, in addition to its high operating speed, is also the possibility of constant and simple correction of the control parameters. The system reads the signals from the engine, camshaft, and crankshaft signals, and uses them and the program variables to generate the control signal for the actuator. For easy management and preview of the current operating parameters of the engine and actuator, a dedicated control and measurement application was designed. The application reads the control system's signals (the position of the crankshaft and camshaft, the position of the accelerator pedal, and others) and displays them on the screen, but it can also be used to change the engine valve's opening and closing times (Figure 10). The essence of the variable compression ratio is the proper opening and closing of the controlled valve. Tests verifying the system's operation were carried out on an electrodynamic dynamometer, which is an equipment owned by the Department of Vehicles at the Opole University of Technology (Figure 11).

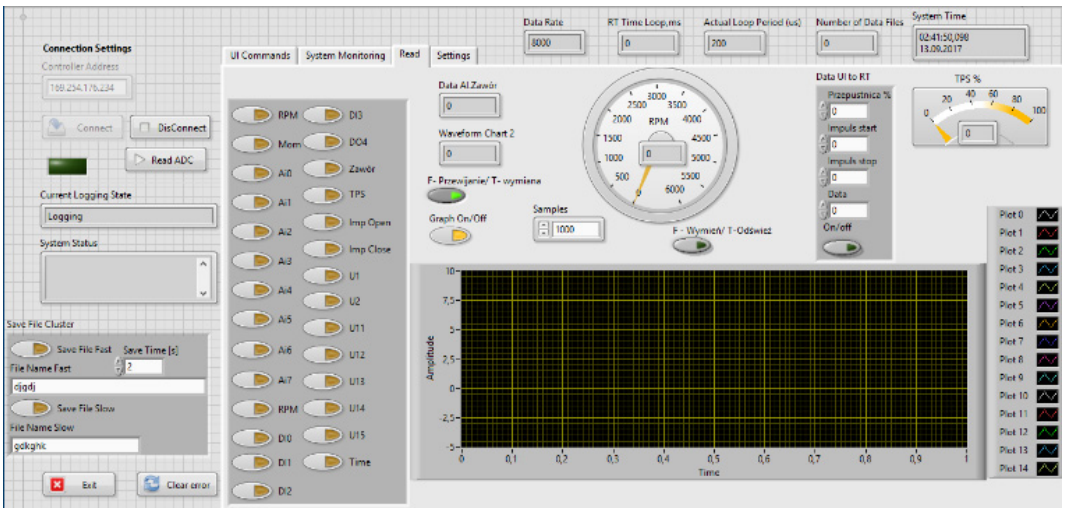

Figure 10. System control application.

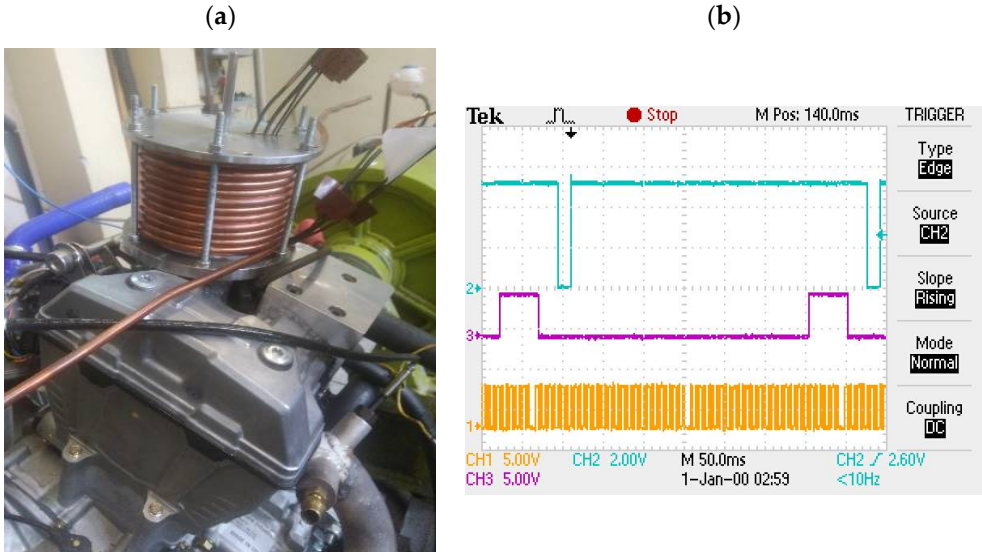

Figure 11. (**a**) Electromagnetic actuator mounted on the engine tested on the dynamometer, (**b**) oscilloscope screen view; yellow—crankshaft, blue—camshaft, purple—valve control signal.

A single cylinder engine type ProStar with indirect injection, spark-ignition engine of 567 cc displacement, 4-stroke, DOHC timing system was used for research purposes. The engine reaches a maximum power of 44 HP at 6700 1/min and generates a maximum torque 49 Nm at 5900 1/min. The basic compression ratio is 9.2:1.

The correct operation of the valve control system was also checked by recording the waveforms from the sensors and the control system with an oscilloscope (Figure 11b). The tests have proved that the proposed electromagnetic actuator, operating with a permanently increased compression ratio, is a good solution, especially at lower crankshaft speeds and engine loads. The electromagnetic actuator's introduction not only increases the engine's power (as shown in Figure 12), but also improves the engine efficiency.

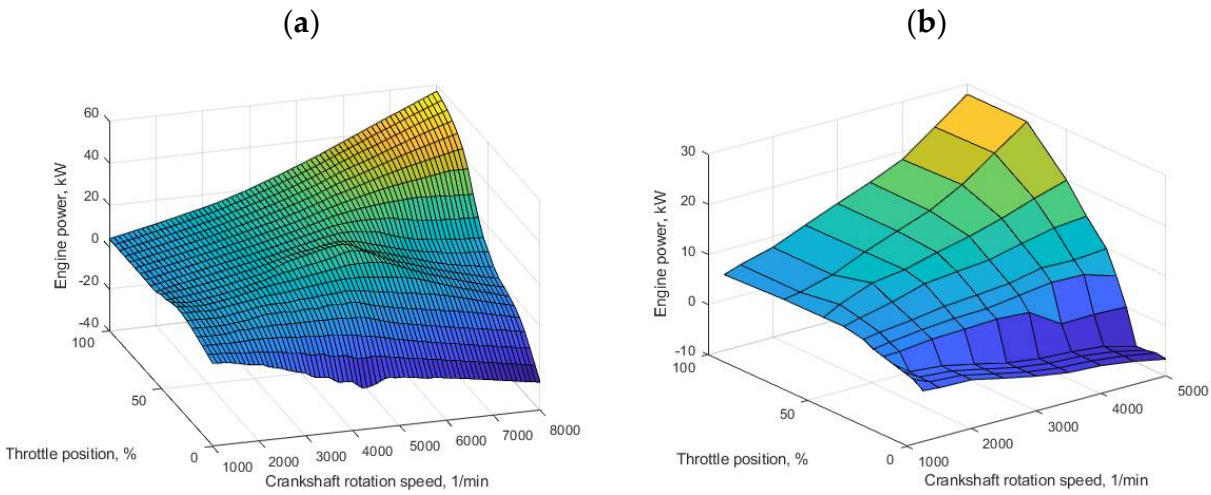

Figure 12. Efficiency characteristics for the tested engine: (**a**) standard engine power, (**b**) modified engine power.

The greatest improvement in power and efficiency is in the part load range of the engine at low engine speed. Engine power in this range increases from 4 kW to 8 kW and fuel consumption is reduced by about 12%. Figure 11b shows the working area in the low-load range and the speed is limited to 5000 rpm. Such changes affect the efficiency of the combustion engine, which is shown in Figure 13.

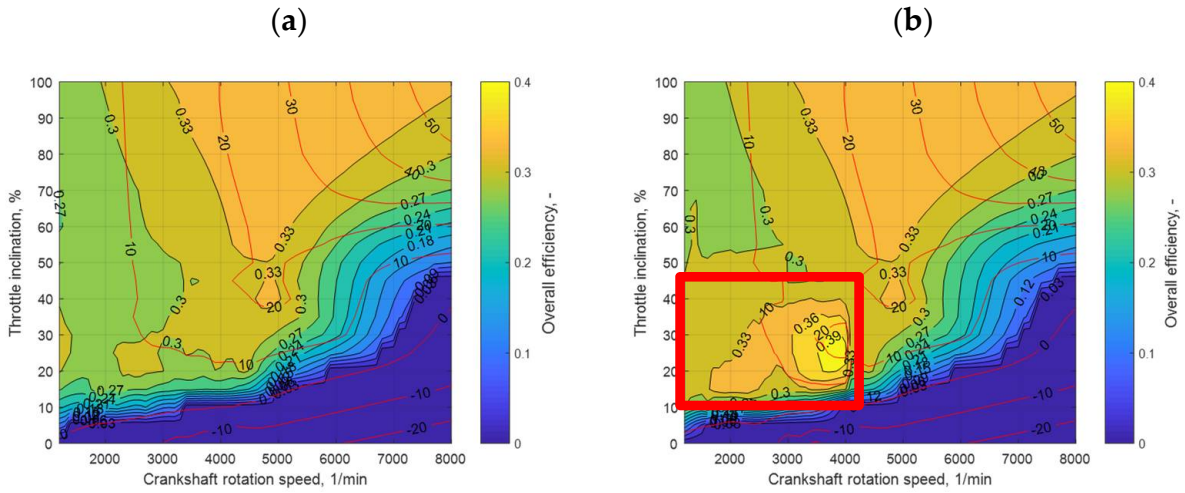

Figure 13. Efficiency characteristics for the tested engine: (**a**) standard engine power with a factory compression ratio (CR 9.2:1); (**b**) modified engine power with an electromagnetic actuator and increased compression ratio (CR 11.5:1).

The presented efficiency characteristics are desirable and efficiency gains are achieved by increasing the effective pressure at constant engine speed and cubic capacity, which are external factors that determine its overall efficiency (highlighted with a square in Figure 13b). In the highlighted area, the engine efficiency increases to 25% and is primarily derived from an improvement in the effective compression ratio in the low-load range, and as the rotational speed increases, the ratio is controlled by the electromagnetic actuator. The analyzed efficiency differences for the electromagnetic actuator constitute a basis for the development of a new ECU engine control algorithm by freeing an additional control space.

6. Conclusions

The first challenge described in this paper was to design an electromagnetic actuator adapted to working in the timing system of internal combustion engines, taking into account its vibrations, temperature and, above all, frequency. The work carried out shows the following:

1. It is advantageous to design DC and control coils with the same widths for the proposed actuator.
2. The desired holding force actuator was ensured by applying a certain current.
3. It is preferable to use the ferromagnetic poles in the form of upper and lower rings with the height h_z = 10 mm. The drive unit's radius should be within the range of R_z = 12 ÷ 14 mm.
4. A ferromagnetic pole should be placed between the upper and lower coils. In the proposed solution, its pole's minimum height should be h_p = 8 mm.

The second challenge was to implement the designed actuator in a combustion engine including its proper controlling. The analyzed electromagnetic actuator is characterized by a new functionality that allows achieving gains in the spark-ignition engine's operating parameters without the need to change its design parameters. The solution also has its limitations related to operating frequency and power consumption. In the case of the proposed effective compression ratio, it is advantageous to increase the ratio at low engine loads. This cannot be achieved through throttles or turbocharging due to the limitations of the combustion process, hence the solution proposed in the paper.

The next important element of the work supplementing its content was the presentation of the effect of using an electromagnetic actuator designed to work in the timing system of an internal combustion engine. In this solution, the modified internal combustion engine is characterized by improved operating parameters at partial loads, including a power increased with simultaneous reduction in fuel consumption, thereby improving

the engine's efficiency by up to 25%. Further work is needed in this regard. The achieved gains translate directly to an improvement in the engine's overall efficiency. It is also worth noting that no engine knocking was observed during the empirical tests. The advantage of using the electromagnetic actuator is its safety and reliability: there is no risk to damage the actuator by the cylinder, which is due to the absence of the mechanical connection between mover and stator.

Further work is needed in this regard. The achieved gains translate directly to an improvement in the engine's overall efficiency. It is also worth noting that no engine knocking was observed during the empirical tests.

Author Contributions: Conceptualization, J.M., B.T. and A.W.; methodology, A.W., J.M. and M.G.; data curation, formal analysis, and simulation, A.W., B.T., M.G. and K.H.; writing—original draft preparation, J.M., A.W. and M.G.; writing—review and editing, A.W., J.M. and M.G.; software, M.G.; Resources, A.W., M.G. and K.H. All authors have read and agreed to the published version of the manuscript.

Funding: This research received no external funding.

Data Availability Statement: The data presented in this study are available on request from the corresponding author.

Acknowledgments: In this work, the authors utilized their experience gained during the implementation of the projects number: RPOP.01.01.00-16-0063/16-00 and RPOP.01.01.00-16-0026/16-00.

Conflicts of Interest: The authors declare no conflict of interest.

References

1. Mamala, J.; Graba, M.; Prażnowski, K.; Hennek cEng, K. *Control of the Effective Pressure in the Cylinder of a Spark-Ignition Engine by Electromagnetic Valve Actuator*; SAE Technical Papers; SAE: Warrendale, PA, USA, 2019; Volume 2019, pp. 1–9. [CrossRef]
2. Urata, Y.; Awasaka, M.; Takanashi, J.; Kakinuma, T.; Hakozaki, T.; Umemoto, A. *A Study of Gasoline-Fuelled HCCI Engine Equipped with an Electromagnetic Valve Train*; SAE Technical Papers Series; SAE: Warrendale, PA, USA, 2004.
3. Rezeka, S.F.; Seddik, E.H.; Abdelghaffar, W.A. Fuzzy Control of a Moving Coil Electromagnetic Valve Actuator for an Automotive Camless Engine. *Int. Rev. Autom. Control* **2014**, *7*, 353. [CrossRef]
4. Theobald, M.A.; Lequesne, B.; Henry, R. *Control of Engine Load via Electromagnetic Valve Actuators*; SAE Technical Papers Series; SAE: Warrendale, PA, USA, 1994.
5. Liu, L.; Chang, S. Improvement of Valve Seating Performance of Engine's Electromagnetic Valvetrain. *Mechatronics* **2011**, *21*, 1234–1238. [CrossRef]
6. Tsai, J.; Koch, C.R.; Saif, M. Cycle Adaptive Feedforward Approach Controllers for an Electromagnetic Valve Actuator. *IEEE Trans. Control Syst. Technol.* **2012**, *20*, 738–746. [CrossRef]
7. Wróblewski, P.; Iskra, A. *Problems of Reducing Friction Losses of a Piston-Ring-Cylinder Configuration in a Combustion Piston Engine with an Increased Isochoric Pressure Gain*; SAE Technical Papers; SAE: Warrendale, PA, USA, 2020. [CrossRef]
8. Wróblewski, P. The Theory of the Surface Wettability Angle in the Formation of an Oil Film in Internal Combustion Piston Engines. *Materials* **2023**, *16*, 4092. [CrossRef] [PubMed]
9. Chen, K.; Zhao, F.; Liu, X.; Hao, H.; Liu, Z. Impacts of the New Worldwide Light-Duty Test Procedure on Technology Effectiveness and China's Passenger Vehicle Fuel Consumption Regulations. *Int. J. Environ. Res. Public Health* **2021**, *18*, 3199. [CrossRef]
10. Lin, J.; Yang, S. A Predictive Study of a New VCR Engine with High Expansion Ratio and High-Efficiency Potential under Heavy Load Conditions. *Energies* **2020**, *13*, 1655. [CrossRef]
11. Mitrovic, J. Optimale Geschwindigkeit von Straßenfahrzeugen Hinsichtlich Des Kraftstoffverbrauchs. *Immissionsschutz* **2020**. [CrossRef]
12. Wurms, R.; Budack, R.; Grigo, M.; Mendl, G.; Heiduk, T.; Knisch, S. The New Audi 2.0l Engine with Innovative Rightsizing—A Further Milestone in the TFSI Technology. In Proceedings of the 36th Vienna Motor Symposium, Vienna, Austria, 7–8 May 2015.
13. Pischinger, S.; Habermann, K.; Yapici, I.Y.; Baumgarten, H.; Kemper, H. Der Weg zum konsequenten Downsizing Motor mit kontinuierlich variablem Verdichtungsverhältnis in einem Demonstrationsfahrzeug. *MTZ-Mot. Z.* **2003**, *64*, 398–405. [CrossRef]
14. Hariram, V.; Vagesh Shangar, R. Influence of Compression Ratio on Combustion and Performance Characteristics of Direct Injection Compression Ignition Engine. *Alex. Eng. J.* **2015**, *54*, 807–814. [CrossRef]
15. Drangel, H.; Olofsson, E.; Reinmann, R. The Variable Compression (SVC) and the Combustion Control (SCC)—Two Ways to Improve Fuel Economy and Still Comply with World-Wide Emission Requirements. In *SAE Transactions*; SAE: Warrendale, PA, USA, 2002.
16. Mishra, R.; Thakare, P.; Patil, S.; Kannav, K.; Vitalkar, N. VC-T Engine An Advancement in 4-Stroke Engine. *Int. J. Eng. Adv. Technol.* **2016**, *8958*, 95–98.

17. Hiyoshi, R.; Aoyama, S.; Takemura, S.; Ushijima, K.; Sugiyama, T. *A Study of a Multiple-Link Variable Compression Ratio System for Improving Engine Performance*; SAE Technical Papers; SAE: Warrendale, PA, USA, 2006. [CrossRef]
18. Ellies, B.; Schenk, C.; Dekraker, P. *Benchmarking and Hardware-in-the-Loop Operation of a 2014 MAZDA SkyActiv 2.0L 13:1 Compression Ratio Engine*; SAE Technical Papers; SAE: Warrendale, PA, USA, 2016. [CrossRef]
19. Sendyka, B.; Sochan, A. Analysis of the Increase of Combustion Engine Total Efficiency with Atkinson Cycle Applied in the Hybrid Driving System. In Proceedings of the FISITA 2006 Congress, Yokohama, Japan, 22–27 October 2006.
20. Mamala, J. Method for Changing the Effective Compression Ratio of an Internal Combustion Engine and System for Changing the Effective Compression Ratio of an Internal Combustion Engine. Patent no. P.414750, 2016. Available online: https://ewyszukiwarka.pue.uprp.gov.pl/search/pwp-details/P.414750 (accessed on 20 June 2023).
21. Duan, J.-A.; Zhou, H.-B.; Guo, N.-P. Electromagnetic Design of a Novel Linear Maglev Transportation Platform with Finite-Element Analysis. *IEEE Trans. Magn.* **2011**, *47*, 260–263. [CrossRef]
22. Lee, H.-W.; Kim, K.-C.; Lee, J. Review of Maglev Train Technologies. *IEEE Trans. Magn.* **2006**, *42*, 1917–1925. [CrossRef]
23. Joseph, D.M.; Cronje, W.A. Design of a Double-sided Tubular Permanent-magnet Linear Synchronous Generator for Wave-energy Conversion. *COMPEL Int. J. Comput. Math. Electr. Electron. Eng.* **2008**, *27*, 154–169. [CrossRef]
24. Tomczuk, B.; Waindok, A.; Wajnert, D. Transients in the Electromagnetic Actuator with the Controlled Supplier. *J. Vibroeng.* **2012**, *14*, 39–44.
25. Bang, Y.-B.; Lee, K.-M. Large Thrust Linear Motors for Low-Duty-Cycle Operation. *Mechatronics* **2004**, *14*, 891–906. [CrossRef]
26. Lee, S.; Yi, H.; Han, K.; Kim, J.H. Genetic Algorithm-Based Design Optimization of Electromagnetic Valve Actuators in Combustion Engines. *Energies* **2015**, *8*, 13222–13230. [CrossRef]
27. Sun, Z.-Y.; Li, G.-X.; Wang, L.; Wang, W.-H.; Gao, Q.-X.; Wang, J. Effects of Structure Parameters on the Static Electromagnetic Characteristics of Solenoid Valve for an Electronic Unit Pump. *Energy Convers. Manag.* **2016**, *113*, 119–130. [CrossRef]
28. Fan, X.; Chang, S.; Liu, L.; Lu, J. Realization and Optimization of High Compression Ratio Engine with Electromagnetic Valve Train. *Appl. Therm. Eng.* **2017**, *112*, 371–377. [CrossRef]
29. Gieras, J.F.; Piech, Z.J.; Tomczuk, B. *Linear Synchronous Motors*; CRC Press: Boca Raton, FL, USA, 2018; ISBN 9781439842225.
30. Boldea, I.; Nasar, S.A. *Linear Electric Actuators and Generators*; Cambridge University Press: Cambridge, UK, 1997; ISBN 9780521480178.
31. Fan, X.; Yin, J.; Lu, Q. Design and Analysis of a Novel Composited Electromagnetic Linear Actuator. *Actuators* **2021**, *11*, 6. [CrossRef]
32. Guo, H.; Liu, L.; Zhu, X.; Chang, S.; Xu, Z. Design of an Electromagnetic Variable Valve Train with a Magnetorheological Buffer. *Energies* **2019**, *12*, 3999. [CrossRef]
33. Shiao, Y.; Kantipudi, M.B.; Weng, C.B. New Actuation Control for Hybrid Electromagnetic Valve Train. *Appl. Sci.* **2022**, *12*, 10449. [CrossRef]
34. Waindok, A.; Tomczuk, B.; Koteras, D. Modeling of Magnetic Field and Transients in a Novel Permanent Magnet Valve Actuator. *Sensors* **2020**, *20*, 2709. [CrossRef] [PubMed]
35. Kawamura, H.; Koza, J. Electromagnetic Valve Actuating System 1991. Available online: https://patents.google.com/patent/US5070826A/en (accessed on 19 June 2023).
36. Mamala, J.T.; Bronisław, W.A. Ferrodynamical Actuator with Permanent Magnets. P.430921/Pat.241833, 2022.
37. Pischinger, M. Reduction of Fuel Consumption and Emissions—Electromechanical Valve Train in Vehicle Operation. *FEV_Spectrum* **1999**. Available online: https://www.fev.com/fileadmin/user_upload/Media/Spectrum/en/spectrum12.pdf (accessed on 15 June 2023).
38. Braune, S.; Liu, S.; Mercorelli, P. Design and Control of an Electromagnetic Valve Actuator. In Proceedings of the 2006 IEEE Conference on Computer Aided Control System Design, 2006 IEEE International Conference on Control Applications, 2006 IEEE International Symposium on Intelligent Control 2006, Munich, Germany, 4–6 October 2006.
39. Hartwig, C.; Josef, O.; Gebauer, K. *Transients of Electromagnetic Valve Train (EMVT) Actuators*; SAE Technical Papers Series; SAE: Warrendale, PA, USA, 2004.
40. Seethaler, R.; Koch, C.R.; Chladny, R.; Mashkournia, M. *Closed Loop Electromagnetic Valve Actuation Motion Control on a Single Cylinder Engine*; SAE Technical Papers Series; SAE: Warrendale, PA, USA, 2013.
41. Shiao, Y.; Dat, L.V. Actuator Control for a New Hybrid Electromagnetic Valvetrain in Spark Ignition Engines. *Proc. Inst. Mech. Eng. Part D J. Automob. Eng.* **2013**, *227*, 789–799. [CrossRef]
42. Mamala, J.; Tomczuk, B.; Waindok, A. Ferrodynamic Servo-Motor and Method of Operation of a Ferrodynamic Servo-Motor. P.425774/Pat.235861, 9 June 2020.
43. Waindok, A. *Modeling and Measurement Verification of Characteristics for the Permanent Magnet Tubular Linear Actuators*; Oficyna Wydawnicza Politechniki Opolskiej: Opole, Poland, 2013.